METSIS: Hyperlocal Wind Nowcasting for U-space

Sun, Junzi; Sunil, Emmanuel ; Koerse, Ralph ; van Selling, Stijn ; van Doorn, Jan-Willem ; Brinkman, Thomas

Publication date
2021

Document Version
Final published version

Published in
11th SESAR Innovation Days

METSIS: Hyperlocal Wind Nowcasting for U-space

Emmanuel Sunil*, Ralph Koerse*,
Stijn van Selling* and Jan-Willem van Doorn†
*ATM and Airports Department
†Vertical Flight and Aeroacoustics Department
Royal Netherlands Aerospace Center (NLR)

Thomas Brinkman
AirHub B.V.

Junzi Sun
Faculty of Aerospace Engineering
Delft University of Technology (TU Delft)

***Abstract*—The METeo Sensors in the Sky (METSIS) project, funded by SESAR's Engage knowledge transfer network, investigated the use of drones as an aerial wind sensor network for U-space applications. The concept aims to provide accurate, low-cost and hyperlocal wind nowcasts for drones using data collected by drones themselves and the Meteo-Particle Model (MPM) for wind field reconstruction. In this paper, we describe the METSIS concept and a proof-of-concept experiment that was performed using four drones to determine the feasibility and accuracy of the concept at low altitudes. For the experiment, ultrasonic anemometers were mounted to each drone to measure local winds. The calibration of the wind sensors was tested using the NLR Anechoic Wind Tunnel. Subsequently, flight-tests were performed at the NLR Drone Center to evaluate the effect of obstacles, drone motion, measurement density, and measurement errors on concept accuracy. Wind fields estimated during the flight-tests were published to the AirHub Drone Operations Center (DOC) system to demonstrate the communication of this data to U-space end-users in real-time. The results indicated that the METSIS concept is a promising solution for the wind nowcast component of the U-space weather information service. Further research is planned to improve the accuracy and sclability of the METSIS concept.**

***Keywords*—U-space; Weather Information Service; Meteo Particle Model (MPM); UTM; Drones**

I. Introduction

Due to their light-weight nature, small drones can be vulnerable to wind. This is particularly true for low altitude operations where both wind speed and direction can change abruptly. However at present, real-time and accurate knowledge of low altitude winds is limited, especially in urban areas. This limitation makes it difficult to safely realize the numerous anticipated applications of drones in urban areas, such as aerial photography, mapping and package delivery.

The SESAR U-space programme, which was established to develop the services needed to integrate drones into European airspace, recognizes this problem. As such, previous SESAR projects have called for the creation of a so called U-space "Weather Information Service" to provide drone operators with information about the actual and forecasted weather situation [1]–[3].

In this context, the METeo Sensors In the Sky (METSIS) project aims to contribute to the wind nowcasting component of the U-space Weather Information Service. Here, the goal is to estimate and communicate hyperlocal wind information to drone operators in real time using (position and meteorological) data measured by the drones themselves, i.e., by using drones as an aerial wind sensor network. In this concept, drones that are already flying measure and transmit the local wind they are experiencing to a ground station. For the proof-of-concept implementation considered in this study, drones were fitted with ultrasonic anemometers that were capable of measuring wind in both horizontal and vertical directions. The ground station aggregates the wind data from the individual drones, and uses the Meteo Particle Model (MPM) to estimate a 3D wind field (vector map) over the sensed area [4], [5]. Subsequently, this data is communicated to drone operators in real time via the U-space Weather Information Service.

Individual drones have been used in the past to reduce the cost and increase the accuracy of atmospheric wind profiling [6]–[10]. The novelty of the METSIS concept is that a *network of drones* are being used to not only measure the wind states at the locations of the drones themselves, but to estimate the 3D wind field within the *area* encompassing the wind measurements using the Meteo-Particle Model (MPM). The resulting *wind field* estimates, which are updated when new measurements are received from individual drones, can be used by drone operators for numerous applications, including for the computation of wind optimized routes to improve mission safety and efficiency (i.e., battery life/range).

To investigate the feasibility of the METSIS concept, NLR and AirHub performed experiments using the NLR Anechoic Wind Tunnel and flight tests at the NLR Drone Center. The wind tunnel experiment considered the accuracy of the selected anemometer when mounted onto the selected quadcopter drone. The flight tests focused on evaluating the effects of obstacles, drone motion, drone density and random measurement errors on the accuracy of METSIS wind estimates. Additionally, the flight tests also considered the communication of wind information to drone operators in real time via the AirHub Drone Operations Center – an active U-space Service Provider (USSP) in the Netherlands.

This paper begins by describing the METSIS concept in section II. Subsequently, details of the wind tunnel experiment and drone flight tests are provided in section III. The results of these experiments are presented and discussed in section IV. Finally, the main conclusions of the METSIS project are summarized in section V.

II. Concept

This section provides an overview of the METSIS concept, considers its advantages and disadvantages, and describes the main working principles of the Meteo-Particle Model (MPM).

A. Concept Overview

The METSIS concept consists of three main steps; see Figure 1. In the first step, instantaneous wind speed and direction measurements are down-linked to the ground by airborne drones. Subsequently in the second step, a ground station aggregates this data, and uses the MPM to estimate a 3D wind field vector map (containing both wind speed and direction at different altitude layers) over a predefined area in real time. This 3D wind field is continuously updated when new wind

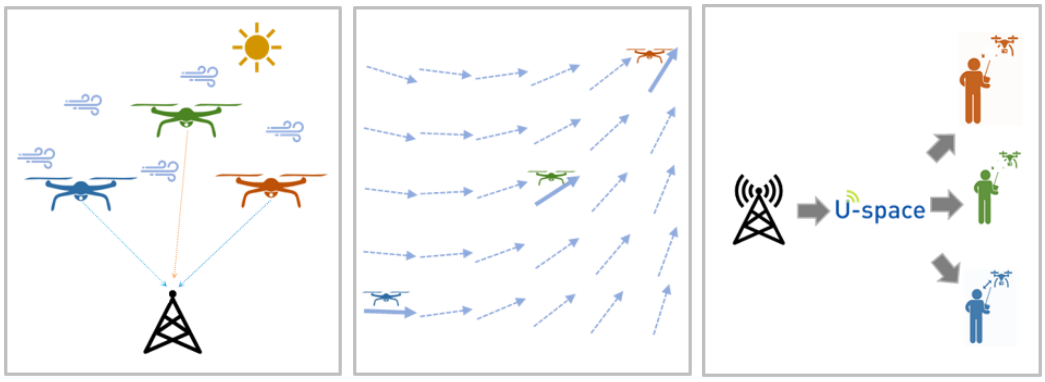

(a) Step 1: Airborne drones measure instantaneous wind states and transmit data to a ground station.

(b) Step2: Ground station uses the Meteo Particle Model (MPM) to estimate the wind field in real time. Here dashed arrows are MPM estimates and solid arrows are drone measurements.

(c) Step 3: The ground station communicates wind field data to drone operators via the U-space weather information service.

Figure 1. The three steps of the METSIS concept.

measurements are transmitted by individual drones to ensure that any wind variations are taken into account.

In the third and final step, the 3D wind field information is communicated to drone operators via the U-space weather information service. For the proof-of-concept flight test performed in this project, wind data was communicated to drone operators through the AirHub Drone Operations Center (DOC). The AirHub DOC makes it possible for drone operators to plan, log and fly missions, and it is an active USSP in the Netherlands. The METSIS ground station used the HTTP POST method to supply the AirHub DOC with updated wind data every 30 seconds. The data was provided in JSON format.

B. Advantages and Disadvantages of the METSIS Concept

The METSIS concept offers several technical and practical advantages. For drone operators, the METSIS approach has the potential to not only improve safety, but also improve flight efficiency as wind can significantly affect drone battery life and range. Additionally, the METSIS concept represents a relatively low-cost solution for wind nowcasting as the drones that are already flying and performing various missions provide the required wind measurements. This further strengths the potential commercialization of the METSIS concept. Beyond drones, this approach for low-altitude wind measurement can also be applied to other use cases, including for Shipboard Helicopter Operational Limitation (SHOL) analysis, safety of construction cranes, and as an additional input to national meteorological forecast systems.

There is, however, one primary limitation of the METSIS concept. Relying on drone measurements for wind nowcasting leads to a 'chicken and egg' problem: wind estimates can only be produced for a particular area once a sufficient number of drones within that area are providing the METSIS ground station with data. This limitation can be mitigated to a large degree by augmenting drone gathered wind measurements with data from ground-based anemometers (e.g. on top of buildings). Although reliance on additional (non-drone) sensors reduces the scalability of the concept, it can increase its availability and overall accuracy, particularly in urban environments with canyon effects in between buildings. It should be noted that the experiment performed in this study does not consider augmenting the METSIS network with ground-based anemometers - but this addition is planned for future implementations. Nonetheless, the current study does provide a preliminary analysis on the effect of the number of drones on wind estimate accuracy; see section IV-B5.

C. Meteo-Particle Model (MPM)

The Meteo-Particle Model (MPM) was originally developed by [5] to estimate high altitude wind fields using ADS-B and Mode-S surveillance data. In the METSIS research, the MPM has been adapted such that it can be used for low altitudes using wind measurements from drones.

The MPM estimates the wind field using a Monte-Carlo approach, where a wind field is assumed to be a pseudo-static over a short timescale. It uses particles to represent wind information derived from aircraft/drone data. These particles propagate in space and time using a Gaussian random walk model. The resulting wind vector for each point of a predefined grid is estimated as the weighted average of the information stored within neighboring particles (taking into account particle age, distance travelled, and distance from the considered grid point). The MPM also computes the confidence level of the wind field estimate at each grid point using the properties of the particles used for the wind field reconstruction.

This data-based approach used by the MPM implies that it will be able to consider the effect of static obstacles, such as buildings and trees, on the wind as long as measurements near such obstacles are provided by the drones. The flight tests performed in this work consider how the accuracy of the system varies with increasing drone distances from static obstacles; see section IV-B3.

The main steps of the MPM are shown in Figure 2. The reader is referred to [5] for a more details on the MPM.

D. MPM Extensions

Close to the ground, two aspects that were not considered in previous implementations of the MPM become increasingly important: the vertical component of wind; and the interaction of the wind with the ground. Because U-space operations are primarily expected in Very Low Level (VLL) airspace (<500 ft), the MPM was modified in this project to take these two aspects into account.

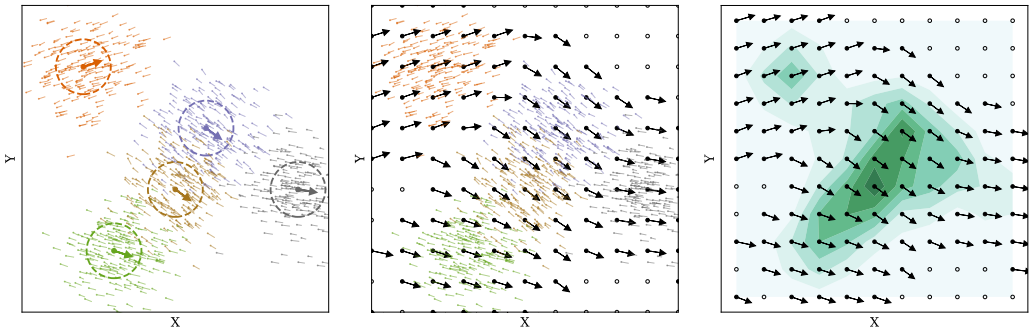

(a) Wind observations and particle initialization (b) Wind field constructed from particles (c) Construction of estimation confidence

Figure 2. Illustration of the Meteo-Particle model key processes [5].

1) Vertical Wind Component
To take into account the vertical component of wind, the underlying MPM algorithms were updated such that particles have both horizontal *and* vertical motion. This primarily affected the particle propagation model of the MPM where a new parameter was introduced to control the vertical motion bias of the particles.

2) Particle-Ground Interaction
An alteration has been made to the way the MPM deals with particles intercepting with the ground. This was done by resetting a particle's altitude to ground level if it drops below the ground during particle propagation. Another option that was considered was to let particles bounce off the ground. This implies keeping the wind speed, but using a 'mirror reflection' of the wind direction compared to the original states stored within a particle. However, this approach would change the information carried by a particle, and as such it violates the stochastic-process underpinnings of the MPM. For this reason, the simpler approach of resetting a particles altitude to ground level was selected for the proof-of-concept implementation tested in this study.

III. Experiment Design

This section describes the goals and the design of the wind tunnel and flight test experiments performed in this study. The primary goal of the experiment was to investigate the feasibility of the METSIS concept.

A. Apparatus

1) Drone
Four Foxtech Hover 1 quadcopter drones were used in this study; see Figure 3. The take-off weight of each drone was about 2.5 kg (batteries and wind sensor included) and has (unfolded) dimensions of 64 × 64 × 28 cm. This drone has a maximum flight duration of 15-20 minutes with the selected battery, and uses the Pixhawk Cube Orange flight controller with two Global Navigation Satellite System (GNSS) receivers and triple-redundant Inertial Measurement Units (IMU). Each drone had its own dedicated ground-control station running the Ardupilot Mission Planner software, and was controlled by one pilot, supported by one observer. Pilots performed take-off and landing, but the rest of the flight was performed using the onboard auto-pilot in order to fly the mission topologies as accurately as possible; see section III-C1.

Two-thirds through the experiment, one of the drones had a crash landing due to a sudden gust of wind. Because of timing constraints, it was decided to continue the last third of the experiment with three drones (two measurement drones and one reference drone; see section III-C1). This mainly affected the second part of the 'Trailer' scenario and the full 'Tree' scenario; see section III-C2. The reader should keep this in mind when considering the results presented here.

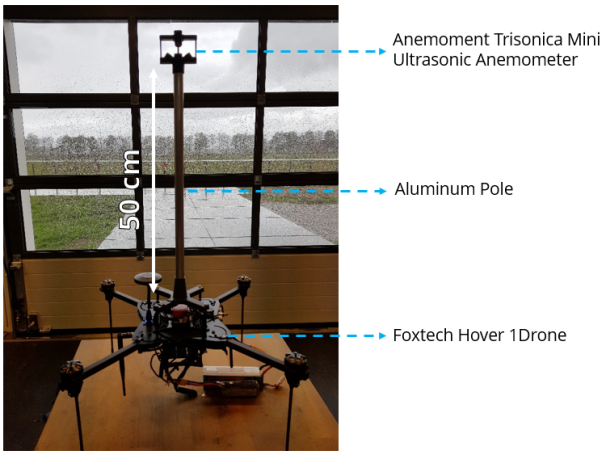

Figure 3. METSIS drone-anemometer configuration.

2) Ultrasonic Anemometer
Anemoment TriSonica Mini ultrasonic anemometers were installed on top of each drone to measure the horizontal and vertical wind vectors in real time. As recommended by previous studies [11], the anemometer was mounted on top of a 50 cm aluminium pole to reduce the effect of propeller induced turbulence on the wind measurement; see Figure 3. The TriSonica Mini has the following manufacturer stated specifications: wind speed range of 0-50 m/s, with an accuracy of ±0.1 m/s for wind speeds between 0-10 m/s. The 3D wind direction range is 360° in the horizontal direction, and 15° for the vertical direction; directional accuracy is ±1° in both directions. These specifications are well within the World Meteorological Organization (WMO) requirements for wind measurement devices [12].

B. Wind Tunnel Experiment Design

An experiment using the NLR Anechoic Wind Tunnel was performed prior to the flight tests; see Figure 4. The goal of the wind tunnel experiment was to analyze the impact of drone propeller rotation and angle of attack (α) on the accuracy of the TriSonica Mini ultrasonic anemometers used in this study. Anemometer accuracy was specifically studied because the anemometers were used during the flight tests to measure the wind states around each drone and to make the measurements needed to determine the accuracy of the METSIS concept. The design of the wind tunnel experiment is described below.

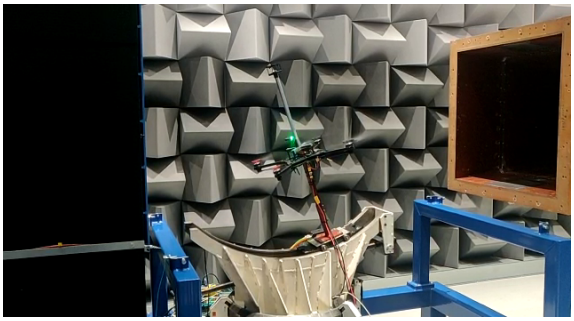

Figure 4. Wind tunnel testing of the Annemoment TriSonica Mini ultrasonic wind sensor mounted on the Foxtech Hover 1 drone.

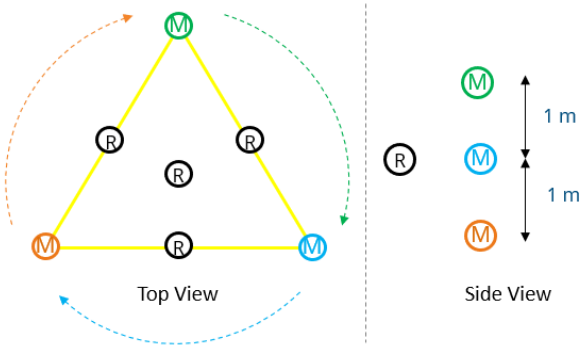

Figure 5. Drone topology used during the flight tests. Note that only the measurement (M) drones moved during dynamic scenarios. The reference (R) drone was always static to improve accuracy computation.

1) Independent Variables

The following independent variables were used for the wind tunnel tests: three wind tunnel speeds (6, 9 and 12 m/s); two drone propeller speeds (0% and 50% corresponding to hover power); and nine angles of attack (α: $-2^o, \ldots, 18^o$, steps of 2.5^o). All combinations of these independent variables were studied, resulting in a total of 54 wind tunnel runs. Each run had a duration of three minutes.

2) Dependent Variables

Accuracy of the TriSonica Mini anemometer was determined by comparing anemometer measurements to those of the flow meters of the wind tunnel. The anemometer measures wind in the body frame. As such, anemometer measurements were converted to the Earth-Centered Earth Fixed (ECEF) reference frame before the comparison was made. Because the air flow in the wind tunnel is tightly controlled and (mostly) horizontal in direction, the horizontal wind speed measured by the anemometer should be (almost) equal to the wind tunnel speed to indicate high anemometer accuracy. In the vertical direction, the wind speed measured by the anemometer should be (almost) zero to indicate high accuracy.

C. Flight Test Design

A one day flight test using four drones was performed at the NLR Drone Center to analyze the effects of static obstacles, drone motion, measurement density and measurement errors on the accuracy of METSIS wind estimates. The following paragraphs describe the design of the flight tests.

1) Drone Topology

The available drones were divided into three 'measurement drones' and one 'reference drone'. The measurement drones were used to establish the METSIS aerial wind sensor network and data from these drones was used by the MPM to estimate the wind field over the experiment area. The reference drone, on the other hand, did not contribute to the network. Instead, it was used to determine the accuracy of the concept. This was done by comparing reference drone wind measurements to the corresponding outputs of the MPM. In other words, reference drone measurements were used as the ground truth for determining concept accuracy during the flight tests. The metric used to assess accuracy is described in section III-C3.

Figure 6. Static obstacles used during the flight tests.

The flight tests employed a predefined topology for both measurement and reference drones to ensure that scenarios could be easily compared with each other; see Figure 5. Here, the measurement drones formed the corners of an equilateral triangle - the 'M' locations in Figure 5. The single reference (R) drone flew between four predefined locations to measure accuracy. Different triangle sizes were performed to consider how distances the between the measurement locations, as well as distances between drones and obstacles, affected accuracy.

During static scenarios, the three measurement drones hovered at the triangle corners. During dynamic scenarios, the measurement drones flew clockwise from corner to corner of the triangle with a constant speed resulting in a circular flight path. The reference drone was always static to provide more accuracy comparisons. A scenario consisted of multiple triangles; see below. An altitude offset of one metre between the measurement drones was used to improve safety, particularly during dynamic scenarios.

2) Independent Variables and Experiment Scenarios

The flight tests considered the following four independent variables: three obstacle types; two drone speeds; three distances between drones (i.e., triangle size); and four altitudes. The resulting experiment scenarios are generated using different combinations of these independent variables are listed in Table I; not all combinations of each independent variable was tested in the experiment. In total, 42 flight test runs were performed over the course of (about) seven hours.

TABLE I
FLIGHT TEST SCENARIOS

#	Obstacle	Triangle Size [m]	Altitude [m]	Speed [m/s]
1	Baseline/None	60,40,20	5,10,20,100	0,3
2	Trailer	60,40,20	5,10	0,3
3	Trees	40	5,10,20	0,3

The 'trailer' and 'trees' obstacles used in the flight test are

displayed in Figure 6. The trailer was placed in the center of the triangular measurement topology. The drones were located 10 meters downstream of the trees in that scenario.

3) Evaluation Metric

The Mean Average Error (MAE) between reference drone measurements and MPM outputs are used to quantify the accuracy of the METSIS concept during the flight tests. The MAE is computed as:

$$MAE = \frac{1}{N}\sum_{i=1}^{N}|e_i - o_i| \quad (1)$$

where N is the number of observations from the reference drone for a specific scenario combination, e are the MPM estimates, and o are the reference drone observed values.

IV. Results and Discussion

The results of the wind tunnel experiment and flight tests are presented and discussed in this section.

A. Wind Tunnel Results

The goal of the wind tunnel experiment was to analyze the effect of drone propeller rotation and drone angle of attack on the accuracy of the TriSonica Mini anemometers used in this study. These anemometers were used in the flight tests to measure the local wind around each drone, and to determine the accuracy of the METSIS wind estimates. The wind tunnel results for the anemometer are displayed in Figure 7. Here, the distance between the second quartile line of the box plots and the actual wind tunnel speed (dashed line) indicates the accuracy, while the distance between the minimum and maximum values of a box plot indicates the variability or precision of the measurements.

From Figure 7, the following conclusions can be drawn:

- The sensor has better performance in the horizontal direction when compared to the vertical direction. The performance in the horizontal direction can be considered to be sufficient. However accuracy is lower than desired in the vertical direction. This affects the utility of the vertical wind measurements made during the flight tests.
- Accuracy degrades with angle of attack in both horizontal and vertical directions. In the horizontal direction, negative angles of attack, which occurs when a quadcopter drone flies forward, has a strong negative influence on accuracy. It is hypothesized that the decrease in accuracy at high and low angles of attack is caused by wind obstruction by the anemometer's frame. More wind tunnel tests are needed to verify this.
- On comparing the 0% to the 50% propeller speeds, it can be seen that propeller induced flows have a significant effect on anemometer measurements in the horizontal direction despite the 50cm pole used to separate the anemometer from the propellers. The results indicate that this is particularly the case at lower wind speeds where propeller induced turbulence has a stronger influence on the airflow around the anemometer, and therefore on anemometer measurements. Because wind speeds during the flight-tests were relatively low ($\leq$ 5 m/s), it is foreseen that accuracy during dynamic conditions, during which propeller speeds are non-constant, will be negatively affected.

In summary, the wind tunnel results indicate that the characteristics of the selected anemometer will have a noticeable impact on the measurements taken during the flight tests. As such, the present flight tests can be used to gain an understanding of the high-level feasibility of the METSIS concept, and to consider the effects of the various scenarios on accuracy in the relative sense. However, the current flight tests can not be used to determine accuracy in the absolute sense.

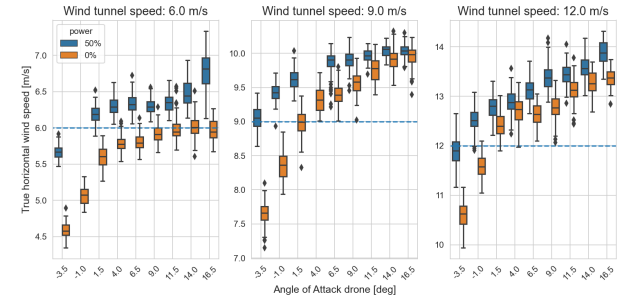

(a) Horizontal Wind Speed

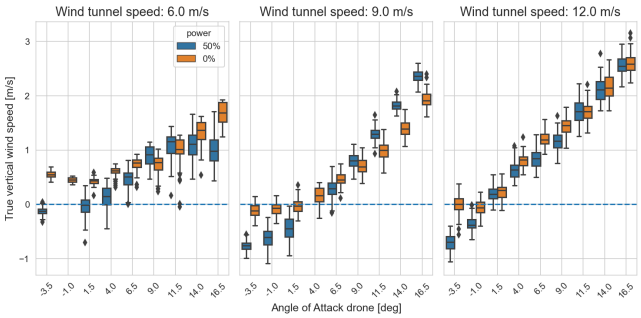

(b) Vertical Wind Speed

Figure 7. Wind tunnel experiment results.

B. Flight Test Results

The goal of the flight tests was to evaluate the overall feasibility of the METSIS concept, and to consider how the accuracy changes as a result of static obstacles, drone motion, measurement density and measurement errors. The results of the flight tests are presented below.

1) Example METSIS Wind Nowcast Output

An example wind nowcast produced by the MPM - corresponding to the second step of the METSIS concept (see Figure 1) - is displayed in Figure 8. This particular nowcast was taken during the trailer scenario, for a triangle size of 60 m and when the drones were at an altitude of 10 meters. Here, each subplot displays the horizontal wind field at a particular altitude. It can be seen that the wind was coming from the south and had a speed ranging between 4.6 m/s at 0 meters to 5.1 m/s at 90 meters altitude. The shade of the green color indicates the estimation confidence levels, where a darker shade indicates a higher confidence. This explains why the altitudes near 10 meters, where the drones were located at this point in time, are marked with a darker shade of green. Similar nowcast figures were also generated for the vertical component of the wind (not shown).

2) Overall Accuracy

Figure 9 displays the Mean Average Error (MAE) results for all scenarios of the flight test. Here, the top subplot considers static runs, while the bottom subplot shows the results for the dynamic runs. Note that the figure has two y-axes. The left y-axis is for wind speed error. The right y-axis is for the wind direction error for both horizontal (XY) and vertical (XZ & YZ) directions. In addition to the MAE, the figure also indicates the mean wind speed per scenario.

The WMO standards for wind measurement devices are [12]:

- Wind speed: ± 0.5 m/s ($\leq$ 5m/s) or 10% ($>$ 5m/s)
- Wind direction: ± 5°

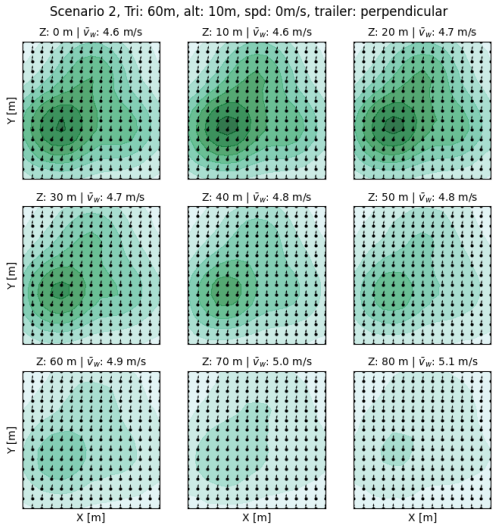

Figure 8. Example METSIS wind nowcast output. This particular nowcast was made during the 'Trailer' scenario.

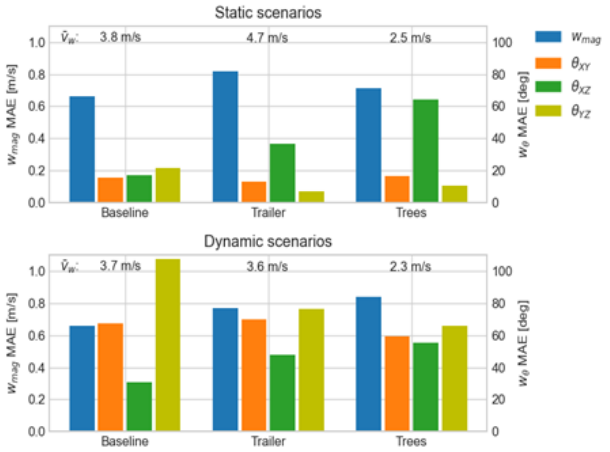

Figure 9. Mean Average Error (MAE) wind speed and direction results for all scenarios of the flight test.

These standards assume the measurement of wind properties at a *single location*. They are not intended to evaluate techniques such as the MPM that estimate the wind over a given *area*. Nonetheless, these standards can be used to gain an initial understanding of the feasibility of the METSIS concept. On comparing the WMO standard to the results in Figure 9, the following main conclusions can be drawn:

- The wind speed MAE is very close to the WMO standard for the baseline scenario during both static and dynamic conditions. The wind speed MAE is larger for the obstacle scenarios, but it is not drastically higher than that for the baseline condition. This indicates reasonably good wind speed estimation performance during the flight tests.
- The wind direction MAE is, on the other hand, far from the WMO standard for all scenarios. Directional accuracy was particularly poor during dynamic runs.

A potential explanation for the poor directional performance mentioned above can be found by analyzing the relationship between the horizontal wind direction error and the average wind speed; see Figure 10. Here, an inverse trend can be seen

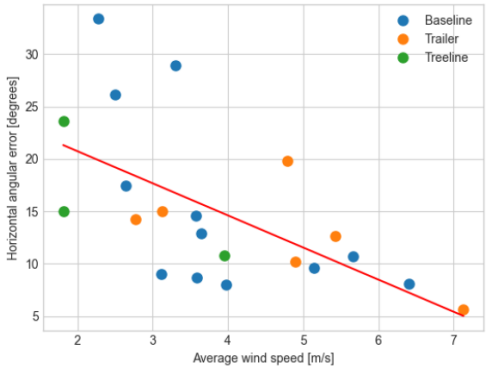

Figure 10. Relationship between average speed and horizontal angular/directional error and the average wind speeds per scenario.

between these two variables, with higher directional error at lower wind speeds. Similar trends were found between the vertical wind direction error and average wind speed (not shown). These trends correlate with some of the wind tunnel results described in section IV-A. There it was shown that effects such as propeller induced turbulence and negative angles of attack (which occur when quadcopter drones fly forward) exacerbate some of the weaknesses of the selected anemometer, especially at low wind speeds. In other words, it is considered highly likely that the poor directional performance can be explained, at least in part, by the deficits of the selected anemometer at low wind speeds. The effect of drone motion during dynamic conditions is further analyzed in section IV-B4.

3) Effect of Static Obstacles on Accuracy

An initial understanding of the effect of obstacles on the MPM accuracy can be gained by comparing the MAE for the baseline scenario with the those of the 'trailer' and 'trees' scenarios where the drones are static; see Figure 11. Here, columns denote different obstacle types, rows represent the different altitudes, and box plot colors represent the triangle sizes (i.e., distances between drones). Additionally, the figure shows the average wind speed under the box plot for each condition in

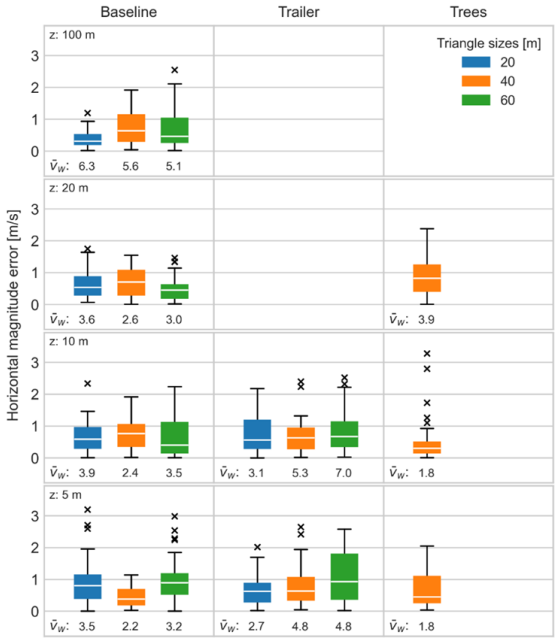

Figure 11. Effect of obstacles on the horizontal wind speed error during static conditions. Note that not all altitudes and triangle sizes were considered for the Trailer and Trees obstacles.

m/s.

From Figure 11, the following main conclusions can be drawn:

- On comparing the average wind speeds for each condition, it is clear that obstacles had a measurable impact on the wind speed, and that wind speed decreases closer to the ground. This effect is most significant for the tree obstacles. This is to be expected as the drones were downstream of the trees, and beneath the tree-line for altitudes less than 15 meters. It should be noted that the drones were always flown above the trailer for safety reasons. It is likely that the wind speed at altitudes below the trailer level would be even more affected than for the tree scenario.
- The box plots for the trailer and tree scenarios overlap with those of the baseline condition. Even though obstacles have a measurable effect on wind speeds as noted above, this result means that the accuracy of the MPM is not significantly affected by obstacles - a positive result for the METSIS concept. This implies that as long as wind measurements are available near obstacles, the effect of obstacles on the wind will be taken into account by the METSIS nowcasts without any significant change in accuracy near obstacles.

The above conclusions are based on horizontal wind speed results. Similar trends were observed for the other dependent variables (vertical wind speed and horizontal/vertical wind direction).

4) Effect of Drone Motion on Accuracy

The effect of drone motion on accuracy can be studied using Figure 12. This figure shows wind nowcasts for three time periods during a dynamic run of the baseline scenario (when the measurement drones were flying a circular flight path with constant speed). Here, the blue arrow is the reference drone measurement and the red arrows are the measurement drone measurements. The black arrows represent the MPM wind field estimates, which are in turn computed using measurement drone data, whereas the green gradient indicates the confidence level of the wind field estimation (darker is better).

Figure 12 indicates close agreement between all three measurement drones (red arrows) and the MPM estimates (black arrows). This suggests that the MPM is working correctly based on the inputs it has been provided. However, there is a significant 90 degree difference between the wind direction measured by the static reference drone (blue arrow) and the dynamic measurement drones (red arrows). Wind socks at the experiment site matched the south-east wind direction measured by the reference drone, indicating a problem with the wind vectors of the measurement drones. Since such a large difference between reference and measurement drones was not found for the static scenarios (when both measurement and reference drones were hovering), this error strongly suggests that the ultrasonic anemometers used here can not reliably measure wind during dynamic conditions. Correspondence with the manufacturer of the anemometer indicated that

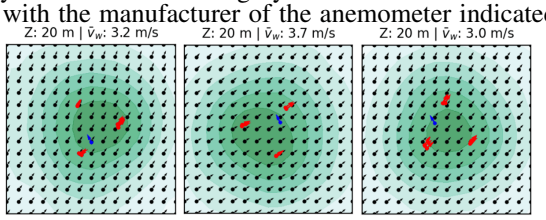

Figure 12. Effect of motion on accuracy. Red arrows: measurement drones, blue arrow: reference drone, black arrows: MPM estimates; Green contour: MPM confidence level.

propeller induced turbulence, which is stronger as a result of asymmetric propeller speeds during dynamic conditions, could be the cause of the erroneous measurements. Similar conclusions were drawn on the basis of the wind tunnel experiment performed in this project; see section IV-A. As such it can be concluded that the current experimental setup is not suitable for investigating the accuracy of METSIS concept during dynamic conditions. This important topic needs to be analyzed further in future studies.

5) Effect of Measurement Density on Accuracy

A qualitative analysis of the effect of measurement density on accuracy can be performed using Figure 13 which shows wind nowcasts for a static baseline run. In this figure, the columns follow a sequential decrease in the number of measurement drones (red arrows) at the same moment in time. This figure was made during post-processing by systematically removing measurement drones from the data set. The rows represent two different reference drone (blue arrow) locations. The black arrows represent the MPM wind field estimates, which are in turn computed using measurement drone data.

In the first row of Figure 13, there are no substantial differences in the nowcast when the number of measurement drones is decreased. However, in the second row of the figure, it is clear that a change of wind direction within the experiment area can only be modeled by the MPM when at least two measurement drones are used. More generally, it can be concluded that the MPM can model changes in the wind field over a particular area only if measurements corresponding to such changes are provided to it. This is a logical conclusion as the MPM is a pure data-based method that does not make any assumptions about the dynamics of the wind. This means that the minimum number of drones needed to establish a METSIS-type nowcasting system depends on the variance of the wind at a particular area and on the desired accuracy level. Nonetheless, it is clear that increasing the number of drones contributing to the network is beneficial for accuracy.

6) Effect of Random Measurement Errors on Accuracy

To gain an initial understanding of the effect of random measurement errors on MPM accuracy, two Gaussian noise models were added to the wind data of all measurement drones for the static baseline runs. Here, the 'low' noise model had a mean of zero and a standard deviation of 0.5 m/s representing 13.1% of the average wind speed during static baseline runs. The 'high' noise model had a mean of zero and a standard deviation of 1 m/s representing 26.2% of the average wind speed. The resulting MAE for the horizontal wind speed is shown in Figure 14 at 5 and 100 meter altitudes . The

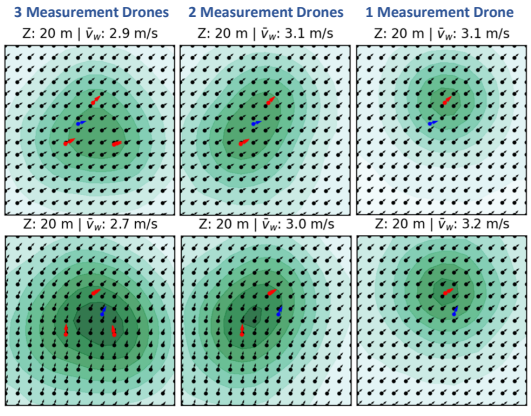

Figure 13. Effect of measurement density on accuracy. Static baseline results shown. Red arrows: measurement drones, blue arrow: reference drone, black arrows: MPM estimates; Green contour: MPM confidence level.

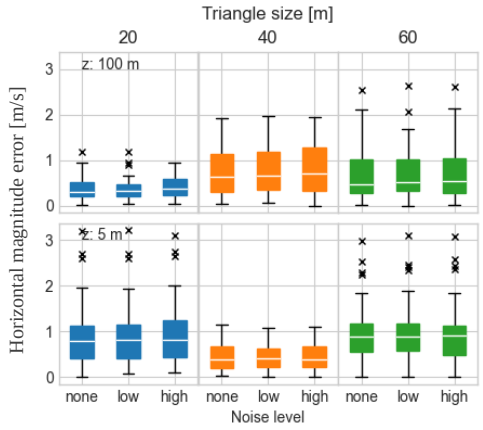

Figure 14. Effect of random measurement noise on accuracy for the static baseline runs at 5 and 100 meter altitudes for all three triangle sizes.

overlapping box plots in the figure indicates that the two noise models had virtually no effect on the accuracy of the MPM (similar trends were found for other altitudes as well as for the vertical wind speed, and for the horizontal/vertical wind directions). This indicates that the probabilistic measurement rejection models of the MPM are capable of accepting or rejecting measurements based on existing particles at the area of measurement without additional tuning [5]. These models ensure that measurements with large errors are excluded from the wind field. This high resilience to random measurement errors ensures that the METSIS concept can be applied on a larger scale at which point such errors become more likely.

V. Conclusions and Recommendations

The METeo Sensors in the Sky (METSIS) project explored the use of drones as an aerial wind sensor network for U-space applications. The novel concept aims to provide accurate and low-cost wind nowcasts for drones using data collected by drones themselves, i.e., "wind nowcasts for drones by drones". In the current incarnation, ultrasonic anemometers were mounted to each drone to measure local winds. The anemometers were studied in a wind tunnel experiment. Subsequently, a proof-of-concept flight-test using four drones was performed to determine the feasibility of the concept at low altitudes. The following main conclusions can be drawn:

- The flight-tests indicated that the METSIS concept is promising and feasible in practice. An implementation on a larger scale could result in a viable and low-cost solution to the hyperlocal wind nowcast component of the U-space weather information service.
- When comparing flight test results to the World Meteorology Organization (WMO) requirements for wind sensors, the concept showed good performance for wind speed estimation.
- However, wind direction accuracy did not meet WMO standards. This deficit was partly due to the low wind speeds experienced during the flight tests which exacerbated some weaknesses of the selected anemometer, as evidenced during the wind tunnel experiment. These deficits also meant that it was not possible to properly analyze the accuracy of the concept when the drones were moving.
- Because METSIS uses a data-based approach, it was shown that the effects of obstacles on wind could be taken into account without affecting accuracy as long as wind measurements are available near obstacles. The method was also shown to be relatively robust against random measurement errors.

Because of the promising results obtained from the flight-tests, it is highly recommended to continue this line of research. The following recommendations are proposed:

- Repeat the experiment over multiple experiment days and consider more experiment scenarios to gain a more thorough understanding of system accuracy.
- Increase the scalability of the concept by investigating indirect wind measurement techniques that do not require a dedicated wind sensor for each drone e.g. by inferring wind from the ground speed and the required propeller RPMs needed to hover or attain a target speed.

Acknowledgements

The authors would like to thank the wind tunnel technicians, drone pilots and observers that took part in this work. The project benefited from the support received from the Engage Knowledge Transfer Network through their Catalyst program. This project has received funding from the SESAR Joint Undertaking under the European Union's Horizon 2020 research and innovation programme under grant No. 783287.

References

[1] SESAR JU, "European ATM Master Plan: Roadmap for the safe integration of drones into all classes of airspace," Tech. Rep., Mar. 2017.

[2] CORUS Consortium, "Concept of Operations for U-space: Enhanced Overview," Tech. Rep. 01.01.03, Sep. 2019. [Online]. Available: https://www.sesarju.eu/node/3411

[3] EASA, "High-level regulatory framework for the U-space," Tech. Rep. Opinion No 01/2020, Mar. 2020.

[4] J. Sun, H. Vû, J. Ellerbroek, and J. Hoekstra, "Ground-based wind field construction from mode-s and ads-b data with a novel gas particle model," in *Proceedings of the Seventh SESAR Innovation Days*, vol. 28, 2017, p. 30th.

[5] J. Sun, H. Vû, J. Ellerbroek, and J. M. Hoekstra, "Weather field reconstruction using aircraft surveillance data and a novel meteo-particle model," *PloS one*, vol. 13, no. 10, p. e0205029, 2018, publisher: Public Library of Science San Francisco, CA USA.

[6] J. D. Jacob, P. B. Chilson, A. L. Houston, and S. W. Smith, "Considerations for atmospheric measurements with small unmanned aircraft systems," *Atmosphere*, vol. 9, no. 7, p. 252, 2018, publisher: Multidisciplinary Digital Publishing Institute.

[7] D. Hollenbeck, M. Oyama, A. Garcia, and Y. Chen, "Pitch and roll effects of on-board wind measurements using sUAS," in *2019 International Conference on Unmanned Aircraft Systems (ICUAS)*. IEEE, 2019, pp. 1249–1254.

[8] W. Thielicke, W. Hübert, U. Müller, M. Eggert, and P. Wilhelm, "Towards accurate and practical drone-based wind measurements with an ultrasonic anemometer," *Atmospheric Measurement Techniques*, vol. 14, no. 2, pp. 1303–1318, Feb. 2021, publisher: Copernicus GmbH. [Online]. Available: https://amt.copernicus.org/articles/14/1303/2021/

[9] C. A. Wolf, R. P. Hardis, S. D. Woodrum, R. S. Galan, H. S. Wichelt, M. C. Metzger, N. Bezzo, G. C. Lewin, and S. F. de Wekker, "Wind data collection techniques on a multi-rotor platform," in *2017 Systems and Information Engineering Design Symposium (SIEDS)*. IEEE, 2017, pp. 32–37.

[10] G. W. Donnell, J. A. Feight, N. Lannan, and J. D. Jacob, "Wind Characterization Using Onboard IMU of sUAS," in *Atmospheric Flight Mechanics Conference*. American Institute of Aeronautics and Astronautics, 2018, _eprint: https://arc.aiaa.org/doi/pdf/10.2514/6.2018-2986. [Online]. Available: https://arc.aiaa.org/doi/abs/10.2514/6.2018-2986

[11] K. Sasaki, M. Inoue, T. Shimura, and M. Iguchi, "In Situ, Rotor-Based Drone Measurement of Wind Vector and Aerosol Concentration in Volcanic Areas," *Atmosphere*, vol. 12, no. 3, p. 376, 2021, publisher: Multidisciplinary Digital Publishing Institute.

[12] World Meteorological Organization, "Part I. Measurement of meteorological variables - Chapter 5: Measurement of surface wind," Tech. Rep., 2014. [Online]. Available: https://library.wmo.int/doc_num.php?explnum_id=3177